THE JOURNAL OF PHYSICAL CHEMISTRY C

Article

pubs.acs.org/JPCC

Spin-Dependent Conductance in Co/C_{60}/Co/Ni Single-Molecule Junctions in the Contact Regime

Xiangmin Fei,[†,‡] Guangfen Wu,[†] Vanessa Lopez,[†] Gang Lu,[†] Hong-Jun Gao,[‡] and Li Gao*[,†]

[†]Department of Physics and Astronomy, California State University, Northridge, California 91330, United States

[‡]Institute of Physics, Chinese Academy of Sciences, Beijing 100190, China

Supporting Information

ABSTRACT: The spin-dependent conductance in Co/C_{60}/Co/Ni single-molecule magnetic tunnel junctions has been measured by combining spin-polarized scanning tunneling spectroscopy and current-displacement measurements using an ultrahigh vacuum low temperature scanning tunneling microscope (STM) at 5 K. With an electrical contact between molecule and electrodes, the measured junction conductance is 0.02−0.13 G_0 in the low-conductance state and 0.12−0.76 G_0 in the high-conductance state, respectively. The investigated single-molecule junctions exhibit large tunnel magnetoresistance (TMR) ratios higher than −60%. A variation of TMR from −63% to −94% has been observed due to different Co/Ni electrodes.

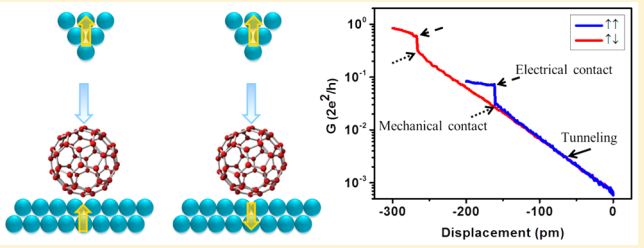

1. INTRODUCTION

Organic molecules are appealing for next-generation spintronic applications due to their weak spin−orbit coupling, weak hyperfine interaction, long electron spin coherence, and chemical diversity.[1−8] Probing and manipulating the spin-dependent electron transport through single molecules is of prime technological importance for the miniaturization of spintronic devices down to molecular scale. Single-molecule magnetic tunnel junctions (MTJs), where two nanometer-scale ferromagnetic electrodes are bridged by a single molecule, are a key component in molecular spintronic devices. Probing the spin-dependent transport in single-molecule MTJs with precisely controlling the molecule-electrode separation is important because the molecule−electrode interface plays a significant role in the injection of spins from magnetic electrodes into molecules.[9] Current versus displacement (I−Z) measurements by scanning tunneling microscope (STM) are capable of detecting the junction conductance as a function of the molecule-electrode separation. In particular, the electrical contact at the molecule−electrode interface can be made and characterized precisely by I−Z measurements.[10−17] Detecting the conductance of junctions in the contact regime is technologically important for their potential applications in high-frequency devices. By using I−Z measurements, the spin-independent conductance in the contact regime has been well investigated for C_{60}-based single-molecule junctions with nonmagnetic electrodes.[10−15] The C_{60} molecule has exhibited a great potential for spintronic applications.[18−25] Therefore, it is of high practical interest to study the electrical contact between a single C_{60} molecule and magnetic electrodes by using I−Z measurements, which has not been reported so far.

Here we report the measurements of spin-dependent conductance in Co/C_{60}/Co/Ni single-molecule MTJs in the contact regime by using an ultrahigh vacuum (UHV) low-temperature STM at 5 K. The junctions were made by approaching the Co-coated Ni STM tip into electrical contact with single C_{60} molecules adsorbed on the Co/Cu(111) surface. Our measurements indicate that the junction conductance ranges from 0.02 G_0 to 0.13 G_0 in the low-conductance state and from 0.12 G_0 to 0.76 G_0 in the high-conductance state, respectively. Tunnel magnetoresistance (TMR) ratios larger than −60% have been observed with three different Co-coated Ni STM tips. The variation of TMR ratios induced by different STM tips is also observed.

2. EXPERIMENTAL SECTION

All the experiments were performed using a Unisoku UHV low temperature STM system with a base pressure lower than 2×10^{-10} Torr. The single crystal Cu(111) surface (Princeton Scientific) was cleaned by repeated cycles of Ar^+ ion sputtering and subsequent annealing. The Co was deposited onto the Cu(111) surface, which was kept at room temperature, from an e-beam evaporator with a Co wire (99.995%, Alfa Aesar). Immediately after Co deposition, the sample was transferred into the STM chamber for fast cooling down to 5 K to avoid the Cu−Co intermixing. The deposition of C_{60} molecules was performed by thermal evaporation from an Al_2O_3 crucible. A thorough degassing of the C_{60} molecules (sublimed grade, 99.9%, Sigma-Aldrich) was performed overnight before

Received: February 22, 2015
Revised: April 7, 2015

DOI: 10.1021/acs.jpcc.5b01763
J. Phys. Chem. C XXXX, XXX, XXX−XXX

molecular deposition. The bulk Ni STM tip was prepared by electrochemically etching of a Ni wire with a diameter of 0.5 mm (≥99.99%, Sigma-Aldrich). The bulk Ni tip was cleaned in UHV by Ar^+ ion sputtering and subsequent annealing before STM measurements. The Co-coated Ni tips with an out-of-plane spin sensitivity were prepared in situ by controlled soft indentations of the Ni tips into the Co islands.[26,27] Scanning tunneling spectroscopy measurements were performed using a lock-in technique with a small ac modulation signal (853 Hz, 20 mV). For $I-Z$ measurements on C_{60} molecules, the STM tip was first stabilized above the molecule with V = +10 mV and I = 500 pA, and then approached toward the molecule while the current was recorded as a function of tip displacement. The gain of the FEMTO current amplifier was set to 10^6 V/A during the $I-Z$ measurements. All the $I-Z$ measurements presented in this paper were performed on the C_{60} molecules adsorbed on the Co islands of the same stacking type (faulted) and size (∼15 nm). In our initial experiments, after molecular deposition, the Co $d_{3z^2-r^2}$ surface state was observed on the faulted islands but not on the unfaulted islands. We speculate that the Co surface state on the unfaulted islands was suppressed by the adsorption of unknown small species (probably hydrogen atoms) coming from the evaporator. For some reason, they preferred to adsorb on the unfaulted islands. So our initial $I-Z$ measurements were performed on the molecules adsorbed on the faulted islands. After further outgassing of the evaporator, however, the Co surface state was observed on both the faulted and unfaulted islands after molecular deposition. Since our initial I-Z measurements were performed on the faulted islands, the same stacking type was chosen in all the I-Z measurements in this work because the electronic structure of the Co islands depends on their stacking type.[28]

3. RESULTS AND DISCUSSION

3.1. Spin-Polarized STM Measurements of Co Islands on Cu(111). Figure 1a shows an STM topography image of Co islands on the Cu(111) surface. Based on stacking and magnetization, four types of Co islands coexist on Cu(111), i.e. unfaulted (↑↑), unfaulted (↑↓), faulted (↑↑) and faulted (↑↓). The faulted and unfaulted Co islands exhibit different geometric orientations, with respect to the underlying Cu(111) surface, and can be distinguished and identified from STM images since the majority of the islands are unfaulted and the minority of them contain a stacking fault.[28] The (↑↑) and (↑↓) Co islands with opposite magnetizations can be distinguished by using a magnetic tip with an out-of-plane magnetization.[16,26−31] Figure 1c shows spin-resolved dI/dV spectra measured on four different types of Co islands marked in Figure 1a. The dominant feature on the dI/dV spectra is a strong occupied peak centered at an energy between −0.28 eV and −0.35 eV below the Fermi energy E_F, corresponding to a spin-polarized Co minority $d_{3z^2-r^2}$ surface state.[28,32,33] Here we designate the parallel (↑↑) and antiparallel (↑↓) alignments based on the alignment of spin-polarization at the bias voltage for the Co $d_{3z^2-r^2}$ surface state (see Supplementary Note 1 in the Supporting Information). The parallel (↑↑) alignment corresponds to the higher dI/dV intensity of the Co $d_{3z^2-r^2}$ surface state, and the antiparallel (↑↓) alignment corresponds to the lower dI/dV intensity of the Co $d_{3z^2-r^2}$ surface state. Similar designations have also been used in previous spin-polarized STM studies.[16,26,28] Figure 1d shows the energy-dependent dI/dV asymmetries arising from opposite magnetizations, which are derived from the spin-resolved dI/dV spectra in Figure 1c. The dI/dV magnetic asymmetry is defined as $A_{dI/dV} = [(dI/dV)_{\uparrow\uparrow} - (dI/dV)_{\uparrow\downarrow}]/[(dI/dV)_{\uparrow\uparrow} + (dI/dV)_{\uparrow\downarrow}]$ and correlated with the spin polarizations of tip and sample $A_{dI/dV} = P_t P_s \cos(\vec{\mathbf{m}}_t, \vec{\mathbf{m}}_s)$. The oscillations between positive and negative values with energy are caused by the sign reversal of the spin-polarization of the tip or the Co islands. Figure 1b shows a dI/dV map recorded at −639 mV for the same region as Figure 1a. Co islands with opposite magnetization directions are clearly distinguishable by dI/dV contrast because the variation of dI/dV intensity at −639 mV is solely induced by the magnetization alignment, as shown in Figure 1c. In addition, the dI/dV map varies with the bias voltage (see Supplementary Figure S1), which is in agreement with the dI/dV spectra in Figure 1c recorded using the same tip.

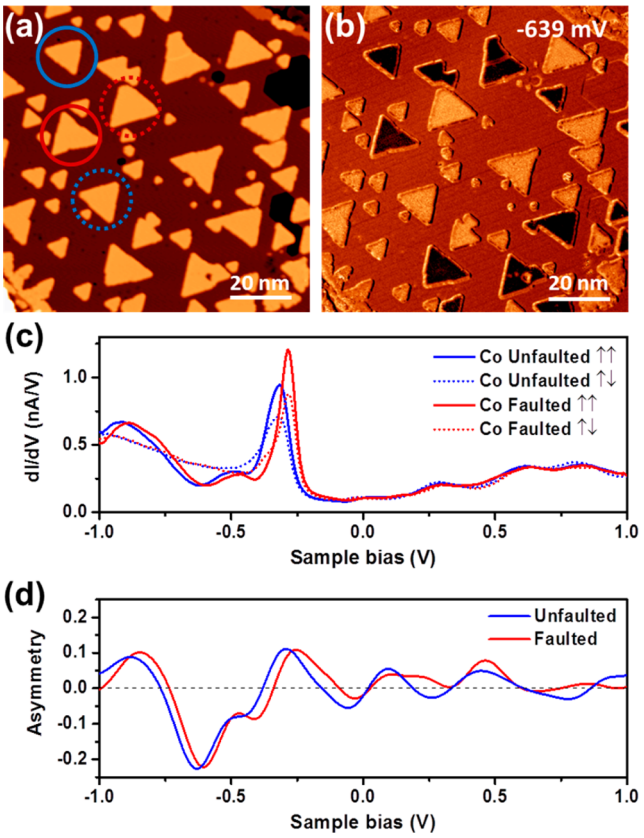

Figure 1. (a) STM topography image of the Cu(111) surface decorated with nanometer-scale Co islands. (b) Spin-resolved dI/dV map at −639 mV. (c) Spin-resolved dI/dV spectra measured on the Co islands indicated in panel a. (d) dI/dV asymmetries arising from opposite magnetizations.

3.2. Spin-Polarized STM Measurements of C_{60}-Decorated Co Islands on Cu(111). With adsorbed C_{60} molecules, the parallel (↑↑) and antiparallel (↑↓) Co islands can still be distinguished by using spin-resolved dI/dV measurements. Figure 2a and 2b are a topography image and a spin-resolved dI/dV map, respectively, of the same region on the sample surface. As the two Co islands, marked as (↑↑) and (↑↓), are of the same stacking type and size, the dI/dV contrast between them arises solely from opposite magnetization alignments. The dI/dV map was recorded at −333 meV, where the dI/dV intensity of the Co $d_{3z^2-r^2}$ surface state is strongly dependent on the magnetization alignment, as shown in Figure 2c. It

DOI: 10.1021/acs.jpcc.5b01763
J. Phys. Chem. C XXXX, XXX, XXX−XXX

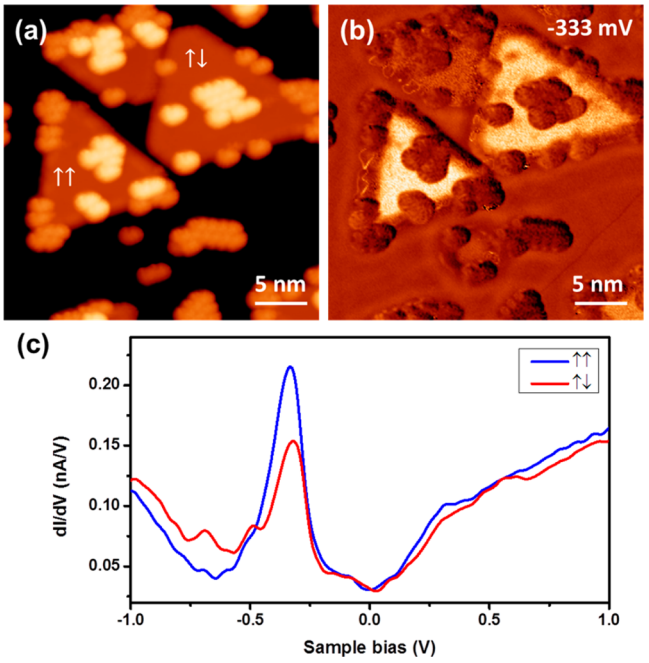

Figure 2. (a) STM topography image of Co islands decorated with C_{60} molecules. (b) Spin-resolved dI/dV map recorded at −333 mV. (c) Spin-resolved dI/dV spectra recorded on the parallel (↑↑) and antiparallel (↑↓) Co islands (faulted) marked in panel a.

should be mentioned that the STM tip used for Figure 2 is different from the one for Figure 1.

3.3. Measurements of Spin-Dependent Conductance in Co/C_{60}/Co/Ni Single-Molecule Junctions. Here we focus on the situation where the molecule is in electrical contact with electrodes, as sketched in Figure 3a. Conductance versus displacement (G−Z) curves were obtained from I−Z curves by calculations using $G = I/V$ (V = 10 mV). Figure 3b shows two representative G−Z curves on a logarithmic scale measured on the C_{60} molecules adsorbed on the parallel (↑↑) and antiparallel (↑↓) Co islands. The unit G_0 is the conductance quantum $G_0 = 2e^2/h$. In the tunneling regime, the conductance varies exponentially with the tip displacement, $G \propto \exp(-1.025\sqrt{\phi}\Delta Z)$, where ϕ is the apparent barrier height and ΔZ is the vertical tip displacement, which corresponds to a linear increase of log $G(Z)$ with increasing tip displacement, as shown in Figure 3b. By fitting the slope of log $G(Z)$ versus ΔZ curves in the tunneling regime, we have determined the value of ϕ and found that it lies between 3 and 7 eV for our over 600 I−Z measurements, which indicates that the tip was clean during the measurements.[34] A Gaussian fit of the obtained ϕ values indicates a statistical ϕ value of 5.12 eV (see Supplementary Figure S2), which is close to the work function (5.0 eV) of Co. The deviation of measured ϕ values from 5.0 eV might be induced by adsorbed molecules.[35,36] The first and second changes in the slope of log $G(Z)$ are induced by mechanical contact and electrical contact, respectively, between the molecule and the tip.[10] Therefore, the conductance of single-molecule junctions in the contact regime can be explicitly determined from the G−Z curves. There are two main differences in spin-dependent transport between the contact and tunneling regimes. First, the spin-dependent transport is

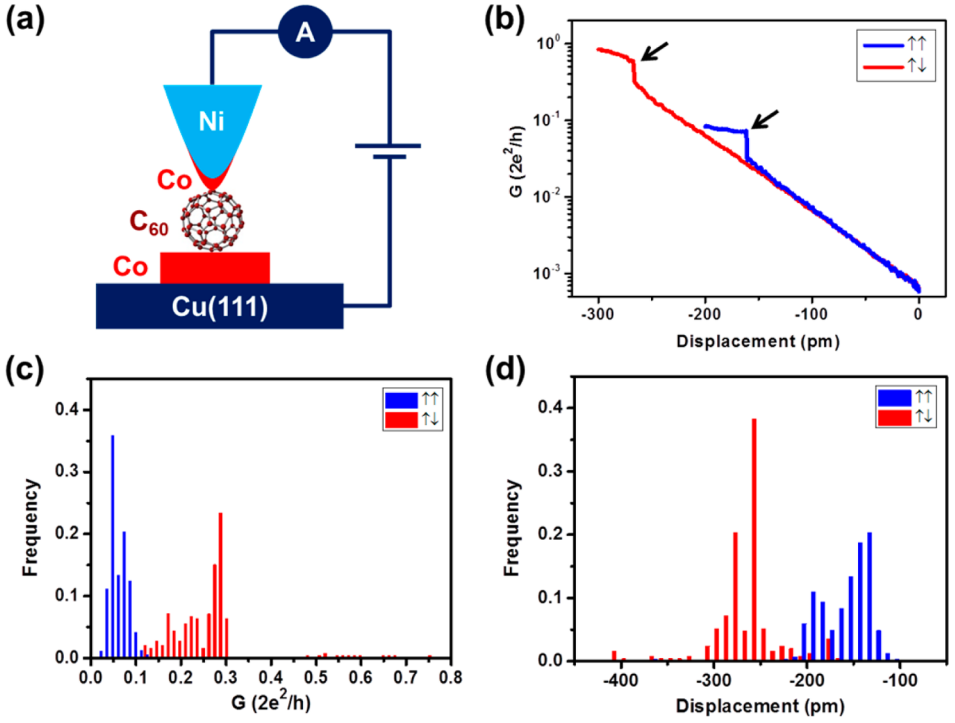

Figure 3. (a) Schematic of the Co/C_{60}/Co/Ni single-molecule junction where the molecule is in electrical contact with electrodes. (b) Two exemplar G−Z curves on a logarithmic scale measured on the C_{60} molecules adsorbed on the parallel (↑↑) and antiparallel (↑↓) Co islands (faulted). The points where electrical contact occurs are indicated by arrows. Stabilization parameters: V = +10 mV, I = 500 pA. (c) Histogram of spin-dependent conductance of the Co/C_{60}/Co/Ni junctions. Data were derived from 710 I−Z measurements (564 ↑↑ and 146 ↑↓) using six different tips. (d) Histogram of spin-dependent tip displacement from the initial stabilization position to the electrical contact position. All the I−Z measurements were performed on the molecules adsorbed on the faulted Co islands.

DOI: 10.1021/acs.jpcc.5b01763
J. Phys. Chem. C XXXX, XXX, XXX−XXX

strongly affected by the spin-polarized hybrid molecular states. In the contact regime, the spin-polarized hybrid molecular states are generated by the interaction between the molecule and both electrodes; while in the tunneling regime the spin-polarized hybrid molecular states are generated by the interaction between the molecule and one electrode, i.e., the Co island. Second, the conductance in the contact regime is significantly higher than that in the tunneling regime. In the following, we focus on the contact conductance at the point where an electric contact just forms between the molecule and the tip, as indicated by the two arrows in Figure 3b.

Figure 3c is a histogram of the measured contact conductance values for the $Co/C_{60}/Co/Ni$ junctions. Our statistics indicates that the contact conductance of the parallel (↑↑) molecular junctions $G_{↑↑}$ is generally lower than that of the antiparallel (↑↓) molecular junctions $G_{↑↓}$. For different tips, $G_{↑↑}$ varies by 1 order of magnitude from 0.02 G_0 to 0.13 G_0 and $G_{↑↓}$ varies approximately by a factor of 7 from 0.12 G_0 to 0.76 G_0. Previous STM studies reported that the spin-averaged contact conductance of C_{60}-based single-molecule junctions is in the range from 0.11 G_0 to 1.55 G_0.[10−15] Figure 3d is a histogram of the tip displacement from the initial stabilization position to the electrical contact position. The vertical tip displacements for the parallel (↑↑) junctions, varying between 90 and 230 pm, are generally smaller than those for the antiparallel (↑↓) junctions, varying between 170 and 410 pm. With the same stabilization parameters, the tip-molecule separation varies with the magnetization alignment between the tip and the sample surface due to spin-polarized electron tunneling.[34]

Electrode geometry and molecular orientation are important factors determining the spin-dependent transport in single-molecule MTJs[17,37,38] as well as the spin-independent transport in single-molecule junctions.[11,12,14,39] As the surfaces of Co islands are all atomically flat and all the islands involved in our measurements are of the same size, the variation of the geometry of Co islands is negligible. The variation of the interaction between the molecule and the Co islands is induced by different molecular orientations. Therefore, the geometry of the tip and molecular orientation are two factors leading to the variations of spin-dependent conductance shown in Figure 3c.

Six different Co-coated Ni tips were used for the measurements in Figure 3. Figure 4a shows the tip-specific histograms of the spin-dependent conductance. For each tip, the dI/dV spectra were measured on the same Co islands before and after I−Z measurements to make sure there was no change to the tip conditions. It is clear that the spin-dependent conductance is strongly dependent on the tips. Among these six tips, three (T2, T4 and T6) were used for measuring the conductance of both parallel (↑↑) and antiparallel (↑↓) junctions. The averaged $G_{↑↓}$ value measured by T2 is around 2 times those measured by T4 and T6. In contrast, the averaged $G_{↑↑}$ values measured by T2 are approximately half of those measured by T4 and T6. The differences between these three tips are reflected by their different geometrical sharpness and spin-polarization. The geometrical sharpness of the tip can be evaluated by the lateral spatial resolution in STM imaging.[40] Figure 5c shows the line height profiles of single C_{60} molecules measured with these three tips. Usually the profile is narrower when the tip is sharper and provides a higher lateral spatial resolution. The profile recorded by T2 is almost the same as that recorded by T4 and is much narrower than that recorded by T6, which indicates that T2 and T4 are much sharper than T6. For STM imaging, T2 and T4 provide much higher lateral spatial

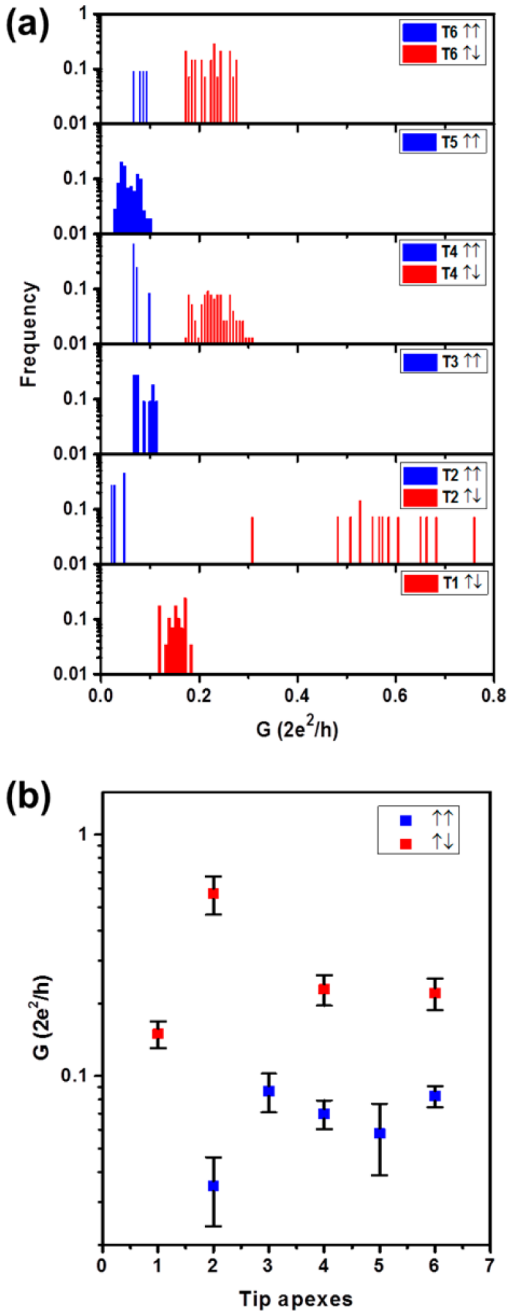

Figure 4. (a) Histogram of spin-dependent conductance measured by six different tips (T1−T6). (b) The averages and standard deviations of the conductance values measured by six different tips (T1−T6). All the data shown here were recorded on the molecules adsorbed on the faulted Co islands.

resolution than T6, as shown in Figure 5c. Recent STM measurements of the $Cu/C_{60}/Cu$ molecular junctions showed that the spin-averaged conductance increases with increasing the number of atoms at the electrode apex, from 0.13 G_0 for single-atom apex to 1.15 G_0 for five-atom apex.[12] However, for the $Co/C_{60}/Co/Ni$ junctions investigated here, increasing the number of atoms on the tip apex does not necessarily lead to an increase of conductance since the spin-polarized electron transport is dominated by the spin-polarization alignment between the molecule and electrodes. Besides the geometrical sharpness, the spin-polarizations of these three tips are also distinctly different from each other, as indicated by the different

DOI: 10.1021/acs.jpcc.5b01763
J. Phys. Chem. C XXXX, XXX, XXX−XXX

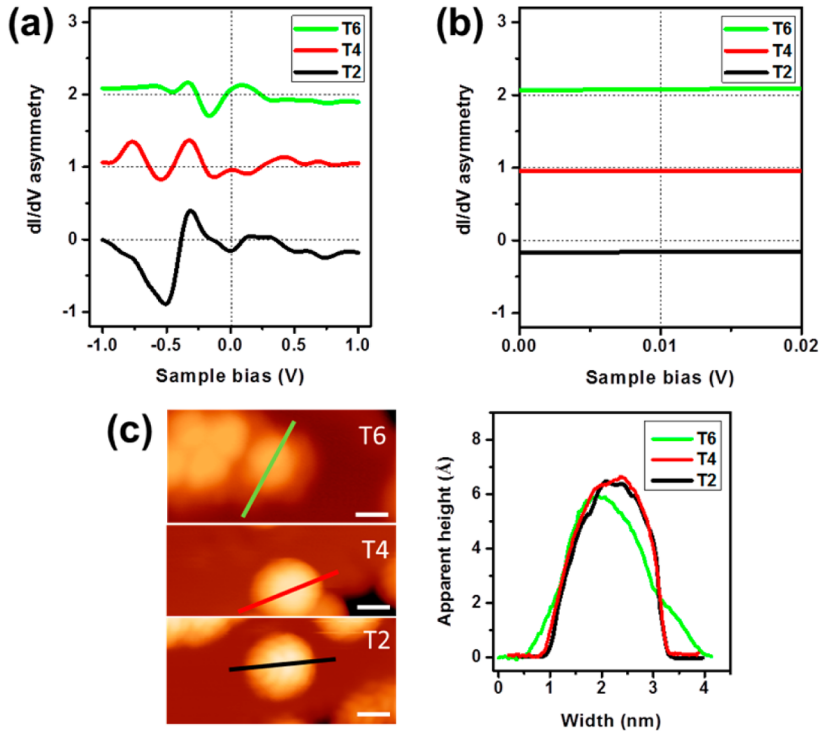

Figure 5. (a) dI/dV magnetic asymmetries of the tips T2, T4, and T6. (b) The zoom-in of panel a for the range of [0, +20 mV] in order to clearly demonstrate the data at +10 mV. (c) STM images of single C_{60} molecules and corresponding line height profiles across the molecule measured by tips T2, T4 and T6. Scale bars, 1 nm. All the data shown here were recorded on the faulted Co islands adsorbed with C_{60} molecules.

dI/dV magnetic asymmetries shown in Figure 5a. It is worth mentioning that the reported dI/dV magnetic asymmetries measured on Co islands on Cu(111) are all different from each other,[26,28−30] which reflects that the spin-polarization of the STM tip apex is very sensitive to its atomic-scale structure. The observed dependence of spin-dependent transport on electrode geometry can exist in single-molecule junctions with other magnetic electrode materials. For example, recent theoretical studies have predicted that the electrode geometry strongly impacts the spin-dependent conductance in Mn(001)/phthalocyanine/Fe and Ni/dithienylethene/Ni single-molecule junctions.[17,38]

For junctions with the same tip, the variations of spin-dependent conductance shown in Figure 4a are induced by different molecular orientations. The junctions with T2 exhibit a broader distribution of conductance compared to the ones with the other tips. The possible reason is that the spin-dependent transport is more sensitive to molecular orientation in the junctions with T2 than in the ones with the other tips. Further measurements under an external magnetic field will allow probing the spin-dependent conductance for each specific molecular orientation.

3.4. Role of C_{60} Molecules in Spin-Polarized Transport in Co/C_{60}/Co/Ni Single-Molecule Junctions. The TMR ratios of Co/C_{60}/Co/Ni junctions, calculated with the definition of TMR = $(G_{\uparrow\uparrow} - G_{\uparrow\downarrow})/G_{\uparrow\downarrow}$, are −94%, −69%, and −63% for tips T2, T4, and T6, respectively. The obtained TMR ratios are close to or even higher than the reported values for C_{60}-based single-molecule MTJs constructed with other electrode materials, for example, −38% and −80% for Ni/C_{60}/Ni junctions,[18,21] and −30% for Fe/C_{60}/Cr junctions.[22] The TMR ratios of Co/Vacuum/Co/Ni junctions, calculated with the definition of TMR = $[(dI/dV)_{\uparrow\uparrow} - (dI/dV)_{\uparrow\downarrow}]/(dI/dV)_{\uparrow\downarrow}$, are −28%, −8% and 17% for T2, T4 and T6, respectively, which are significantly lower than those of corresponding Co/C_{60}/Co/Ni junctions. In addition, for junctions constructed with T6, the C_{60} molecules even lead to the sign reversal of the TMR. The observed enhancement and sign reversal of the TMR clearly indicate that the C_{60} molecule plays a crucial role in the spin-polarized electron transport through the molecular junctions. For T2- and T4-based junctions, the C_{60} molecule significantly enhances the magnitude of the TMR while keeping its sign unchanged. In contrast, for T6-based junctions, the C_{60} molecule not only enhances the magnitude of the TMR but also reverses its sign. The observed strong dependence of TMR ratio on the tips can be ascribed to two primary reasons. First, different tip apexes exhibit various spin-polarizations, as evidenced by the recorded dI/dV magnetic asymmetries in Figure 5a. Second, the spin-polarized hybrid molecular states, induced by molecule−electrode interactions, are strongly dependent on the atomic structure of the tip apex. Our DFT calculations of the Co/C_{60}/Co junctions show that the spin-polarized local density of states of the C_{60} molecule varies substantially when just one Co atom is removed from the tip apex (see Supplementary Figure S3).

The molecule-induced magnitude enhancement and sign reversal of the TMR ratio can be qualitatively understood using the model that has been put forward by Barraud et al. for the (La,Sr)MnO_3/Alq_3/Co molecular junctions.[41] At a certain bias voltage V, the electronic states involved in the electron transport in the junctions are within the energy range defined by the two dashed lines sketched in Figure 6. When the molecule and the electrodes are in electrical contact, the molecular energy levels are broadened and shifted due to their electronic coupling to the electronic states of electrodes.[42] First, when the tip is not in electrical contact with the C_{60} molecule,

DOI: 10.1021/acs.jpcc.5b01763
J. Phys. Chem. C XXXX, XXX, XXX−XXX

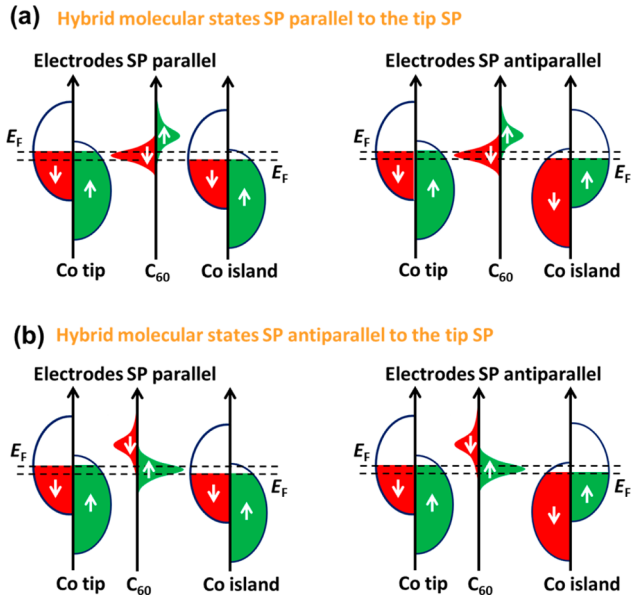

Figure 6. Possible mechanisms for the enhancement and sign reversal of the TMR induced by the C_{60} molecule. (a) The spin-polarization (SP) of the hybrid molecular states is parallel to that of the tip, in which case the C_{60} molecule enhances the magnitude of the TMR while keeping the sign of the TMR unchanged. (b) The spin-polarization of the hybrid molecular states is antiparallel to that of the tip, in which case the C_{60} molecule reverses the sign of the TMR. For the configurations on the left in panels a and b, the spin-polarizations of the tip and the Co island are parallel to each other, and for the configurations on the right in panels a and b, the spin-polarizations of the tip and the Co island are antiparallel to each other.

the electronic structure of the molecule is affected only by the Co islands. It is well-known that the molecule−substrate interaction can broaden and shift the energy levels of C_{60} molecules when they are adsorbed on transition metal surfaces.[43,44] Such phenomena have also been observed in our dI/dV measurements of C_{60} molecules on the Co islands. Our measurements indicate that the molecular energy levels are broad, and the lowest unoccupied molecular orbital (LUMO) is near the Fermi energy E_F (see Supplementary Figure S4). The observed shift of LUMO toward the E_F indicates charge transfer from the Co islands to the C_{60} molecule, which is in agreement with recent X-ray magnetic circular dichroism measurements for C_{60} molecules adsorbed on Co thin films.[44] Second, when the tip is in electrical contact with the C_{60} molecule, the electronic structure of the molecule is affected by both the tip and the Co islands. The hybridization between the Co 3d states of both electrodes and the LUMO of the C_{60} molecule generates hybrid molecular states. As both electrodes are ferromagnetic, the hybrid molecular states are spin-polarized. The spin-polarized hybrid molecular states act as electron spin-filters and strongly impact the electron transport process through the molecular junctions. As the electronic coupling between the molecule and the tip is dependent on the atomic-scale structure of the tip apex, the hybrid molecular states vary with different tip apexes. Figure 6 shows possible mechanisms for magnitude enhancement and sign reversal of the TMR ratio induced by the C_{60} molecule. If the spin-polarization of the hybrid molecular states is parallel to that of the tip within the related energy range, as shown in Figure 6a, the spin-filtering effect induces a more significant decrease of conductance for the antiparallel configuration than for the parallel configuration, in which case the C_{60} molecule enhances the TMR while keeping its sign unchanged. If the spin-polarization of the hybrid molecular states is antiparallel to that of the tip within the related energy range, as shown in Figure 6b, the spin-filtering effect induces a more significant decrease of conductance for the parallel configuration than for the antiparallel configuration, in which case the C_{60} molecule leads to a sign reversal of TMR. The actual energy level alignment at the molecule/electrode interfaces can be calculated if the atomic structure of the tip apex is known, which is not within the scope of this paper. In addition, the TMR ratio of T2-based molecular junctions is much higher than those of T4- and T6-based molecular junctions, which may stem from the fact that, near the Fermi energy E_F, T2 has much larger spin-polarization than the other two tips, as indicated by the dI/dV magnetic asymmetries in Figure 5a.

4. SUMMARY AND CONCLUSIONS

In summary, we have measured the spin-dependent conductance in Co/C_{60}/Co/Ni single-molecule MTJs in the contact regime. With an electrical contact between the molecule and electrodes, the junction conductance is 0.02−0.13 G_0 for the low-conductance state and 0.12−0.76 G_0 for the high-conductance state. Large TMR ratios higher than −60% have been observed. The observed variation of TMR induced by electrode geometry indicates that atomic-scale engineering of the electrode apex is important for high-yield fabrication of single-molecule MTJs with reproducible characteristics.

■ ASSOCIATED CONTENT

Supporting Information

Additional spin-resolved dI/dV maps of Co islands on Cu(111), histogram of ϕ values, DFT calculations of spin-polarized local density of states of the C_{60} molecule in Co/C_{60}/Co junctions, dI/dV spectra of the C_{60} molecule adsorbed on the Co/Cu(111) surface, and the designation of parallel (↑↑) and antiparallel (↑↓) alignments between the Co-coated Ni tip and the Co islands. The Supporting Information is available free of charge on the ACS Publications website at DOI: 10.1021/acs.jpcc.5b01763.

■ AUTHOR INFORMATION

Corresponding Author

*E-mail: li.gao@csun.edu. Tel: 1-818-677-4365. Fax: 1-818-677-3234.

Notes

The authors declare no competing financial interest.

■ ACKNOWLEDGMENTS

We gratefully acknowledge financial support from California State University, Northridge, and the National Science Foundation (NSF) under Grant DMR-1205734.

■ REFERENCES

(1) Dediu, V. A.; Hueso, L. E.; Bergenti, I.; Taliani, C. Spin Routes in Organic Semiconductors. *Nat. Mater.* **2009**, *8*, 707−716.

(2) Pramanik, S.; Stefanita, C.-G.; Patibandla, S.; Bandyopadhyay, S.; Garre, K.; Harth, N.; Cahay, M. Observation of Extremely Long Spin Relaxation Times in an Organic Nanowire Spin Valve. *Nat. Nanotechnol.* **2007**, *2*, 216−219.

(3) Ouyang, M.; Awschalom, D. D. Coherent Spin Transfer between Molecularly Bridged Quantum Dots. *Science* **2003**, *301*, 1074−1078.

DOI: 10.1021/acs.jpcc.5b01763
J. Phys. Chem. C XXXX, XXX, XXX−XXX

(4) Dediu, V.; Murgia, M.; Matacotta, F. C.; Talianli, C.; Barbanera, S. Room Temperature Spin Polarized Injection in Organic Semiconductor. *Solid State Commun.* **2002**, *122*, 181−184.
(5) Xiong, Z. H.; Wu, D.; Vardeny, Z. V.; Shi, J. Giant Magnetoresistance in Organic Spin-Valves. *Nature* **2004**, *427*, 821−824.
(6) Shim, J. H.; Raman, K. V.; Park, Y. J.; Santos, T. S.; Miao, G. X.; Satpati, B.; Moodera, J. S. Large Spin Diffusion Length in an Amorphous Organic Semiconductor. *Phys. Rev. Lett.* **2008**, *100*, 226603(1−4).
(7) Santos, T. S.; Lee, J. S.; Migdal, P.; Lekshmi, I. C.; Satpati, B.; Moodera, J. S. Room-Temperature Tunnel Magnetoresistance and Spin-Polarized Tunneling through an Organic Semiconductor Barrier. *Phys. Rev. Lett.* **2007**, *98*, 016601(1−4).
(8) Petta, J. R.; Slater, S. K.; Ralph, D. C. Spin-Dependent Transport in Molecular Tunnel Junctions. *Phys. Rev. Lett.* **2004**, *93*, 136601(1−4).
(9) Sanvito, S. The rise of spinterface science. *Nat. Phys.* **2010**, *6*, 562−564.
(10) Joachim, C.; Gimzewski, J. K.; Schlittler, R. R.; Chavy, C. Electronic Transparence of a Single C_{60} Molecule. *Phys. Rev. Lett.* **1995**, *74*, 2102−2105.
(11) Schull, G.; Frederiksen, T.; Brandbyge, M.; Berndt, R. Passing Current through Touching Molecules. *Phys. Rev. Lett.* **2009**, *103*, 206803(1−4).
(12) Schull, G.; Frederiksen, T.; Arnau, A.; Sánchez-Portal, D.; Berndt, R. Atomic-Scale Engineering of Electrodes for Single-Molecule Contacts. *Nat. Nanotechnol.* **2011**, *6*, 23−27.
(13) Frederiksen, T.; Foti, G.; Scheurer, F.; Speisser, V.; Schull, G. Chemical Control of Electrical Contact to sp^2 Carbon Atoms. *Nat. Commun.* **2014**, *5*, 3659(1−7).
(14) Néel, N.; Kröger, J.; Limot, L.; Berndt, R. Conductance of Oriented C_{60} Molecules. *Nano Lett.* **2008**, *8*, 1291−1295.
(15) Néel, N.; Kröger, J.; Limot, L.; Frederiksen, T.; Brandbyge, M.; Berndt, R. Controlled Contact to a C_{60} Molecule. *Phys. Rev. Lett.* **2007**, *98*, 065502(1−4).
(16) Schmaus, S.; Bagrets, A.; Nahas, Y.; Yamada, T. K.; Bork, A.; Bowen, M.; Beaurepaire, E.; Evers, F.; Wulfhekel, W. Giant Magnetoresistance through a Single Molecule. *Nat. Nanotechnol.* **2011**, *6*, 185−189.
(17) Bagrets, A.; Schmaus, S.; Jaafar, A.; Kramczynski, D.; Yamada, T. K.; Alouani, M. b.; Wulfhekel, W.; Evers, F. Single Molecule Magnetoresistance with Combined Antiferromagnetic and Ferromagnetic Electrodes. *Nano Lett.* **2012**, *12*, 5131−5136.
(18) Yoshida, K.; Hamada, I.; Sakata, S.; Umeno, A.; Tsukada, M.; Hirakawa, K. Gate-Tunable Large Negative Tunnel Magnetoresistance in Ni−C_{60}−Ni Single Molecule Transistors. *Nano Lett.* **2013**, *13*, 481−485.
(19) Sakai, S.; Sugai, I.; Mitani, S.; Takanashi, K.; Matsumoto, Y.; Naramoto, H.; Avramov, P. V.; Okayasu, S.; Maeda, Y. Giant Tunnel Magnetoresistance in Codeposited Fullerene-Cobalt Films in the Low Bias-Voltage Regime. *Appl. Phys. Lett.* **2007**, *91*, 242104(1−3).
(20) Sakai, Y.; Tamura, E.; Toyokawa, S.; Shikoh, E.; Lazarov, V. K.; Hirohata, A.; Shinjo, T.; Suzuki, Y.; Shiraishi, M. Observation of Magnetic-Switching and Multiferroic-Like Behavior of Co Nanoparticles in a C_{60} Matrix. *Adv. Funct. Mater.* **2012**, *22*, 3845−3852.
(21) Pasupathy, A. N.; Bialczak, R. C.; Martinek, J.; Grose, J. E.; Donev, L. A. K.; McEuen, P. L.; Ralph, D. C. The Kondo Effect in the Presence of Ferromagnetism. *Science* **2004**, *306*, 86−89.
(22) Kawahara, S. L.; Lagoute, J.; Repain, V.; Chacon, C.; Girard, Y.; Rousset, S.; Smogunov, A.; Barreteau, C. Large Magnetoresistance through a Single Molecule due to a Spin-Split Hybridized Orbital. *Nano Lett.* **2012**, *12*, 4558−4563.
(23) Gobbi, M.; Golmar, F.; Llopis, R.; Casanova, F.; Hueso, L. E. Room-Temperature Spin Transport in C_{60}-Based Spin Valves. *Adv. Mater.* **2011**, *23*, 1609−1613.
(24) Tran, T. L. A.; Le, T. Q.; Sanderink, J. G. M.; van der Wiel, W. G.; de Jong, M. P. The Multistep Tunneling Analogue of Conductivity Mismatch in Organic Spin Valves. *Adv. Funct. Mater.* **2012**, *22*, 1180−1189.
(25) Zhang, X.; Mizukami, S.; Kubota, T.; Ma, Q.; Oogane, M.; Naganuma, H.; Ando, Y.; Miyazaki, T. Observation of a Large Spin-Dependent Transport Length in Organic Spin Valves at Room Temperature. *Nat. Commun.* **2013**, *4*, 1392(1−7).
(26) Iacovita, C.; Rastei, M. V.; Heinrich, B. W.; Brumme, T.; Kortus, J.; Limot, L.; Bucher, J. P. Visualizing the Spin of Individual Cobalt-Phthalocyanine Molecules. *Phys. Rev. Lett.* **2008**, *101*, 116602(1−4).
(27) Heinrich, B. W.; Iacovita, C.; Rastei, M. V.; Limot, L.; Ignatiev, P. A.; Stepanyuk, V. S.; Bucher, J. P. A Spin-Selective Approach for Surface States at Co Nanoislands. *Eur. Phys. J. B* **2010**, *75*, 49−56.
(28) Pietzsch, O.; Kubetzka, A.; Bode, M.; Wiesendanger, R. Spin-Polarized Scanning Tunneling Spectroscopy of Nanoscale Cobalt Islands on Cu(111). *Phys. Rev. Lett.* **2004**, *92*, 057202(1−4).
(29) Corbetta, M.; Ouazi, S.; Borme, J.; Nahas, Y.; Donati, F.; Oka, H.; Wedekind, S.; Sander, D.; Kirschner, J. Magnetic Response and Spin Polarization of Bulk Cr Tips for In-Field Spin-Polarized Scanning Tunneling Microscopy. *Jpn, J. Appl. Phys.* **2012**, *51*, 030208(1−3).
(30) Oka, H.; Ignatiev, P. A.; Wedekind, S.; Rodary, G.; Niebergall, L.; Stepanyuk, V. S.; Sander, D.; Kirschner, J. Spin-Dependent Quantum Interference within a Single Magnetic Nanostructure. *Science* **2010**, *327*, 843−846.
(31) Yayon, Y.; Brar, V. W.; Senapati, L.; Erwin, S. C.; Crommie, M. F. Observing Spin Polarization of Individual Magnetic Adatoms. *Phys. Rev. Lett.* **2007**, *99*, 067202(1−4).
(32) Diekhöner, L.; Schneider, M. A.; Baranov, A. N.; Stepanyuk, V. S.; Bruno, P.; Kern, K. Surface States of Cobalt Nanoislands on Cu(111). *Phys. Rev. Lett.* **2003**, *90*, 236801(1−4).
(33) Rastei, M. V.; Heinrich, B.; Limot, L.; Ignatiev, P. A.; Stepanyuk, V. S.; Bruno, P.; Bucher, J. P. Size-Dependent Surface States of Strained Cobalt Nanoislands on Cu(111). *Phys. Rev. Lett.* **2007**, *99*, 246102(1−4).
(34) Wiesendanger, R.; Güntherodt, H.-J.; Güntherodt, G.; Gambino, R. J.; Ruf, R. Observation of Vacuum Tunneling of Spin-Polarized Electrons with the Scanning Tunneling Microscope. *Phys. Rev. Lett.* **1990**, *65*, 247−250.
(35) Rusu, P. C.; Brocks, G. Work Functions of Self-Assembled Monolayers on Metal Surfaces by First-Principles Calculations. *Phys. Rev. B* **2006**, *74*, 073414(1−4).
(36) de Boer, B.; Hadipour, A.; Mandoc, M. M.; van Woudenbergh, T.; Blom, P. W. M. Tuning of Metal Work Functions with Self-Assembled Monolayers. *Adv. Mater.* **2005**, *17*, 621−625.
(37) Saffarzadeh, A. Tunnel Magnetoresistance of a Single-Molecule Junction. *J. Appl. Phys.* **2008**, *104*, 123715(1−5).
(38) Ulman, K.; Narasimhan, S.; Delin, A. Tuning Spin Transport Properties and Molecular Magnetoresistance through Contact Geometry. *J. Chem. Phys.* **2014**, *140*, 044716(1−8).
(39) Ulrich, J.; Esrail, D.; Pontius, W.; Venkataraman, L.; Millar, D.; Doerrer, L. H. Variability of Conductance in Molecular Junctions. *J. Phys. Chem. B* **2006**, *110*, 2462−2466.
(40) Tersoff, J.; Hamann, D. Theory of the Scanning Tunneling Microscope. *Phys. Rev. B* **1985**, *31*, 805−813.
(41) Barraud, C.; Seneor, P.; Mattana, R.; Fusil, S.; Bouzehouane, K.; Deranlot, C.; Graziosi, P.; Hueso, L.; Bergenti, I.; Dediu, V.; Petroff, F.; Fert, A. Unravelling the Role of the Interface for Spin Injection into Organic Semiconductors. *Nat. Phys.* **2010**, *6*, 615−620.
(42) Rocha, A. R.; García-suárez, V. M.; Bailey, S. W.; Lambert, C. J.; Ferrer, J.; Sanvito, S. Towards Molecular Spintronics. *Nat. Mater.* **2005**, *4*, 335−339.
(43) Shi, X.-Q.; Van Hove, M.; Zhang, R.-Q. Survey of Structural and Electronic Properties of C_{60} on Close-Packed Metal Surfaces. *J. Mater. Sci.* **2012**, *47*, 7341−7355.
(44) Moorsom, T.; Wheeler, M.; Khan, T. M.; Ma'Mari, F. A.; Kinane, C.; Langridge, S.; Ciudad, D.; Bedoya-Pinto, A.; Hueso, L.; Teobaldi, G.; et al. Spin-Polarized Electron Transfer in Ferromagnet/C_{60} Interfaces. *Phys. Rev. B* **2014**, *90*, 125311(1−6).

DOI: 10.1021/acs.jpcc.5b01763
J. Phys. Chem. C XXXX, XXX, XXX−XXX